minerals

MDPI

Review

Case Histories of Orogenic Gold Deposits

Franz Michael Meyer

Institute of Applied Mineralogy and Economic Geology, RWTH Aachen University, Wüllnerstrasse 2, 52056 Aachen, Germany; m.meyer@rwth-aachen.de

Abstract: This review compares genetic parameters of 12 orogenic gold deposits. The set of examples is considered to represent largely the variability of orogenic gold deposit (OGD) characteristics. The data are presented in tables and include following definitive parameters: regional geologic settings, nature of hosts rocks and mineralization, ore controlling structures, ages of host rocks and mineralization and timing of mineralization relative to metamorphism, hydrothermal alteration mineralogy and ore mineral assemblages, isotopic signatures, physical conditions of ore formation and proposed origin of ore fluids aa well as gold reserves, production, and grades. This allows comparison of deposits from different geologic terrains having different ages and formed under different P-T conditions. The data are further discussed before the background of the orogenic gold system and the crustal metamorphic models that provide different scenarios to explain the source of ore fluids. The orogenic gold system model advocates a metal and fluid source external to the terrain in which mineralization occurred, but the model applies only for 3 of the 12 deposits studied. All other deposits formed most likely from a crustal source, which would favor the crustal metamorphic model. However, the formation of hypozonal OGDs cannot be accounted for by the crustal metamorphic model or by the metamorphic devolatilization model. The data identify a set of coherent signatures in OGDs, but there seem to be no unified model for all possible environmental conditions and facets of ore formation and fluid sources, tectonic and lithologic setting, and scale of gold endowment.

Keywords: orogenic gold deposits; hydrothermal fluid chemistry; models for the source of ore fluids

Citation: Meyer, F.M. Case Histories of Orogenic Gold Deposits. *Minerals* **2023**, *13*, 369. https://doi.org/10.3390/min13030369

Academic Editors: Vasilios Melfos, Panagiotis Voudouris and Grigorios Aarne Sakellaris

Received: 16 January 2023
Revised: 19 February 2023
Accepted: 20 February 2023
Published: 6 March 2023

1. Introduction

This paper reviews research on orogenic gold deposits (OGD) carried out by staff and students at the Institute of Mineralogy and Economic Geology, RWTH Aachen University. A large body of research is documented in formal publications as well as MSc and PhD theses so that this review paper can only showcase some of the many aspects related to the gold deposits that were studied.

The section on Materials and Methods is purposely lacking, as all information on regional and mine geology, host rock and ore sample descriptions, as well as analytical methods such as litho- and mineral chemical and petrological analyses, fluid inclusion studies, stable and radiogenic isotope analyses, and petrological modeling are provided in the references cited below.

Data for the review originate from research projects involving following mines and mining districts (in order of decreasing mineralization ages). References pertaining to individual ore deposits discussed are indicated in square brackets: New Consort, South Africa [1–9]: Cuiabá Brazil [10–13]: Ajjanahalli, India [14,15]; Renco, Zimbabwe [16–20]; Hutti [21–27], Hira Buddini [28,29], India; Pilgrim's Rest [30–33], South Africa; Lega Dembi, Ethiopia [34]; Navachab, Namibia [35–40]; Mindyak [41–43], Kochkar [44–46], Russia; Awak Mas, Indonesia [47–53].

Processes of formation of orogenic gold systems have been well studied and the salient features are thoroughly documented [54–58]. With the recognition of diagnostic criteria and based on an adequate theoretical basis it is widely accepted that orogenic gold

deposits represent structurally controlled hydrothermal deposits that formed by focused fluid flow in an orogenic setting during metamorphism and deformation [54–59]. The crustal continuum model has been one of the generally accepted descriptive models for OGDs formation in Archaean greenstone belts [56,57]. The model proposes that OGDs formed along crustal faults over an extended range of pressure and temperature conditions throughout a 20–25 km vertical profile, from temperatures ranging from below 180 °C to above 700 °C. Mineralization occurred synchronous with the peak of metamorphism extending from sub-greenschist to lower granulite facies conditions [56,57]. The crustal continuum model was mainly based on the observation of systematic variations of mineralization and alteration features in the vertical crustal profile. Accordingly, shallow-level gold deposits were classified as epizonal, intermediate-level deposits as mesozonal, and the deep-seated deposits as hypozonal [56]. Since hypozonal deposits commonly form in mid-amphibolite or lower-granulite terrains the crustal continuum model requires the existence of a deep source for the ore fluids [57]. The metamorphic devolatilization model was invoked to explain the fluid source in greenstone-hosted gold deposits [60]. In this model, ore fluids are generated by metamorphic devolatilization in an orogenic setting of hydrated and carbonated metabasic rocks across the greenschist–amphibolite facies boundary [60,61]. Further work on hypozonal orogenic gold deposits suggests that the crustal continuum model is not valid over the large spectrum of temperatures and pressures of OGD formation. Additionally, the metamorphic devolatilization model fails to explain the formation of OGDs at metamorphic conditions of the host terrane above the greenschist to amphibolite facies transition [1,62]. Alternative models consider external sources of fluids and gold such as devolatilization of a subducted oceanic slab with its overlying gold-bearing sulfide-rich sedimentary package, or release from mantle lithosphere that was metasomatized and fertilized during a subduction event, particularly adjacent to craton margins [59]. Enhanced asthenopsheric heat input, typical of an unstable or delaminated subcontinental lithospheric mantle, promotes the devolatilization of sedimentary and/or volcanic rocks that produce metamorphic fluids in well-endowed gold provinces [63–65].

This paper reviews distinctive signatures, on a deposit scale, of 12 selected OGDs. The data are presented in tables and include following definitive characteristics: regional geologic settings, nature of hosts rocks and mineralization controlling structures, ages of host rocks and mineralization and timing of mineralization relative to metamorphism, hydrothermal alteration mineralogy and ore mineral assemblages, isotopic signatures, physical conditions of ore formation and proposed origin of ore fluids as well as gold reserves, production, and grades. This allows comparison of deposits from different geologic terrains having different ages and formed under different P-T conditions.

2. Geologic Setting and Mineralization Characteristics

The geographical spread of OGDs studied is shown in Figure 1. Four deposits are situated in southern Africa, three in India, two in Russia, one in Ethiopia, Brazil and Indonesia. The geographic diversity also points to diverse geologic settings that host the OGDs as summarized in Table 1.

The nature of host formations is diverse on regional scales. New Consort, Cuiabá, Hutti, Ajjanahalli, Hira Buddini and Lega Dembi are situated in greenstone belts, Renco formed in a granulite facies mobile belt, Pilgrim's Rest is hosted by Proterozoic platform carbonates, Navachab is in the Pan African Damara orogen, Mindyak and Kochkar formed as consequence of the Uralian orogeny, and Awak Mas is hosted by the Upper Cretaceous Latimojong Formation.

There is common acceptance that the formation of OGDs is structurally controlled [57]. Most deposits shown in Table 2 are located along major compressional to transtensional crustal-scale fault zones in deformed greenstone terranes. Gold mineralization, in general, is localized in lower order structural traps such as moderately to steeply dipping, compressional brittle-ductile shear zones, reverse faults, shallow-dipping extensional veins, and tubular sheath folds [56]. As an exception, Ajjanahalli is situated within a first-order

shear zone and at Kochkar the ore-bearing shear zones are developed along granite-mafic dyke contacts in the Plast Granite. The Pilgrim's Rest host structures are shallow dipping, bedding-parallel thrust faults located at the contact between interbedded carbonaceous shale layers and carbonate host rocks.

Figure 1. Geographic distribution of gold deposits studied.

Table 1. Regional geologic settings of hosts to the OGDs.

Deposit	Regional Geologic Settings
New Consort	Barberton Greenstone Belt
Cuiabá	Rio das Velhas Supergroup (Nova Lima Group)
Ajjannahalli	West Dhawar Craton (Chitradurga Greenstone Belt)
Renco	Limpobo Belt (Northern Marginal Zone)
Hutti	East Dhawar Craton (Hutti-Maski Greenstone Belt)
Hira Buddini	East Dhawar Craton (Hutti-Maski Greenstone Belt)
Pilgrim's Rest	Transvaal Supergoup (Malmani Subgroup)
Lega Dembi	Megado belt (Adola Granite-Greenstone Terrane)
Navachab	Damara Belt (Southern Central Zone)
Mindyak	Main Uralian Fault Zone (Magnitogorsk Megazone)
Kochkar	East Uralian Zone (Plast Granite Massif)
Awak Mas	Latimojong Formation

Important for triggering gold precipitation is the rheological behavior of the host-rock assemblage [58]. Failures of more competent rocks provide specific permeability for fluid migration and fluid-rock reaction. Hydraulic fracturing and pressure cycling between supralithostatic to hydrostatic pressure results in fluid immiscibility and gold precipitation. Fluid reaction with Fe-rich host rocks leads to gold deposition via sulfidation reactions as well as fluid reduction in carbon-rich sedimentary host rocks [63]. As shown in Table 3, gold precipitation does not require an association with one specific rock type. Ore-bearing hosts are mafic and ultramafic volcanic rocks, Fe-rich gabbroic dykes, carbonaceous siliclastic metasedimentary rocks and banded iron formation. Renco is an example of an unusual setting in that it is hosted by discrete mylonites developed in an Enderbite intrusion. Irrespective of the nature of host rocks, gold mineralization is predominantly confined to (often laminated) quartz-carbonate vein networks or may be present within Fe-rich sulfurized wall rock selvages or silicified and arsenopyrite-rich replacement zones.

Table 2. Mineralization controlling structures.

Deposit	Host Structure
New Consort	Consort Bar shear zone
Cuiabá	Cuiabá tubular sheath fold
Ajjanahalli	Chitradurga boundary shear zone
Renco	North Limpopo thrust zone (high-T mylonite zone)
Hutti	Hutti-Maske shear zone (high-angle shear zone system)
Hira Buddini	Reverse shear zone
Pilgrims's Rest	Shallow dipping thrust faults
Lega Dembi	Lega-Dembi-Aflata shear zone
Navachab	Mon Repos thrust zone
Mindyak	Strike-slip fault zones (Main Uralian Fault)
Kochkar	Shear zones at mafic dike-granitoid contacts
Awak Mas	Oblique normal faults, extensional shears

Table 3. Host rocks to the gold mineralization.

Deposit	Host Rock Lithology
New Consort	Mafic-ultramafic volcanics
Cuiabá	Algoma-type BIF, mafic volcanics
Ajjanahalli	Oxide-, Carbonate-facies BIF
Renco	Enderbite
Hutti	Amphibolite, felsic schist
Hira Buddini	Metabasalt, metagabbro, metadacite
Pilgrim's Rest	Carbonaceous shale, gabbroic sills
Lega Dembi	Graphitic meta-sediments
Navachab	Marble, calc-silicates, biotite shist
Mindyak	Fe-rich diabase, carbonaceous shale
Kochkar	Mafic dykes, granitoid
Awak Mas	Carbonaceous phyllites and shists

The ages of host lithologies and related mineralization are summarized in Figure 2. Mineralization ages range from the Mesoarchean (New Consort) to Phanerozoic times (Awak Mas). The distribution of ages is not continuous as this data set reveals a gap over 1500 Ma between the Paleoproterozoic Pilgrim's Rest district and the Neoproterozoic Lega Dembi and Navachab deposits. Most of the greenstone-hosted OGDs in Figure 2 are of Neoarchean age while Mindyak, Kochkar and Awak Mas formed during Phanerozoic times.

Deposits hosted by collisional or accretionary orogenic belts, commonly formed at peak to post-peak metamorphism (Table 4) at the waning stage of tectonism that produced the orogenic belt [59]. Mineralization at Cuiabá, Ajjanahalli, Renco, Hutti, Hira Buddini, Lega Dembi, Navachab, Mindyak and Kochkar is between 5 Ma (Navachab) and up to 90 Ma (Ajjanahalli) younger than the host rock. The time age gaps are even larger for New Consort (245 Ma), Pilgrim's Rest (245 Ma), and Awak Mas (114 Ma).

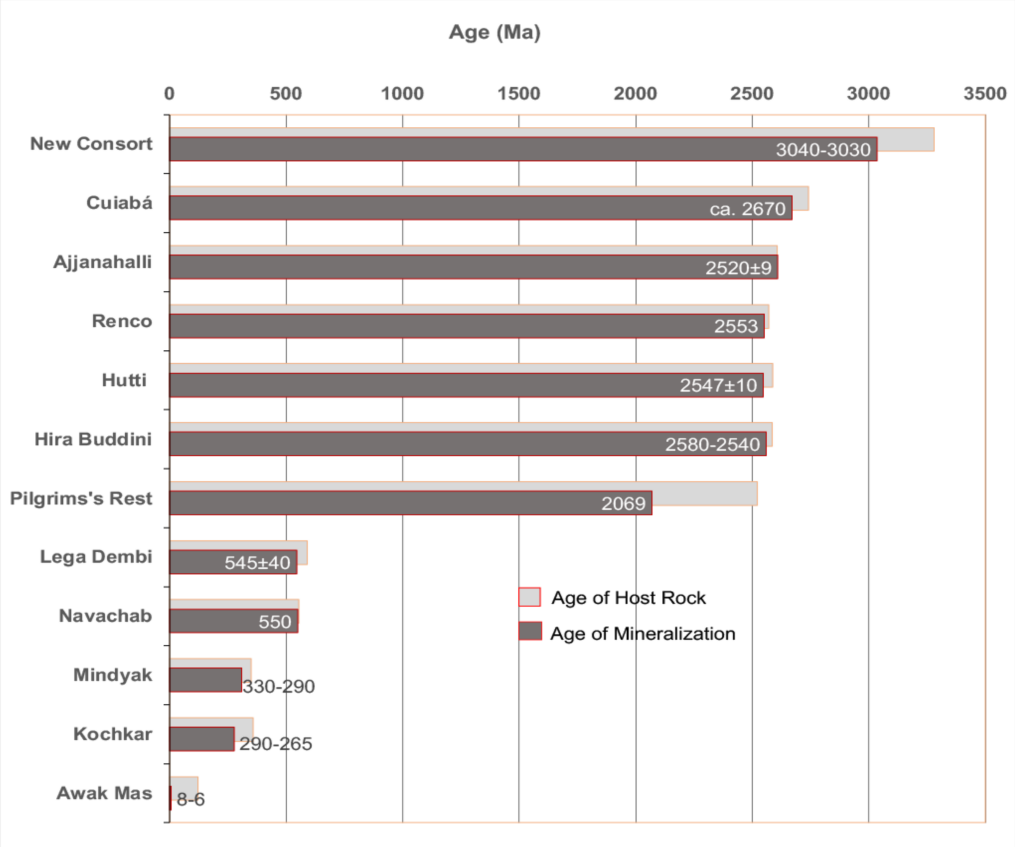

Figure 2. Ages of host rocks and mineralization.

Table 4. Timing of mineralization relative to metamorphism.

Deposit	Timing Relative to Metamorphism
New Consort	2 stages, post-peak metamorphism
Cuiabá	syn- to late-peak metamorphism
Ajjanahalli	post-peak metamorphism
Renco	post-peak metamorphism
Hutti	2 stages, post peak metamorphism
Hira Buddini	2 stages, post peak metamorphism
Pilgrim's Rest	post metamorphism
Lega Dembi	syn- to late-peak metamorphism
Navachab	2 stages, syn-peak metamorphism
Mindyak	post-peak metamorphism
Kochkar	peak-metamorphism
Awak Mas	post metamorphism

In the case of New Consort, the tectonic processes responsible for gold mineralization, most likely, were external to the greenstone belt. Asthenospheric heat input resulted from instability or delamination of the subcontinental lithospheric mantle as consequence of crustal accretion and convergence along the edges of the Kaapvaal Craton [1–9]. This promoted a crustal architecture composed of a craton-wide period of granite plutonism and associated low-P, high-T metamorphism. The resulting thermal disequilibrium was causative for the devolatilization of sedimentary and/or volcanic rocks at deeper crustal

levels, that produced the ore-bearing metamorphic fluids [1–9]. At Renco fluids were derived from thrusting of the granulite facies Northern Marginal Zone of the Limpopo Belt over the greenstone terrane of the Zimbabwe Craton, whereby the latter suffered prograde metamorphism and dehydration [16–20].

Gold mineralization at Pilgrim's Rest may also be related to an external process such as the intrusion of the Bushveld Igneous Complex into the sediments of the Transvaal Supergroup at 2069 Ma [30–33]. The regional metamorphic grade of the Malmani Subgroup is sub-greenshist facies, however, amphibole occurs close to the contact with the Bushveld Complex [30–33]. From the Awak Mass deposit, a spatial relationship is recorded with a granodiorite intrusion into the flysch-type metasediments of the Upper Cretaceous Latimojong Formation dated at 8–6 Ma, but a genetic relationship is unclear [47–50]. In some instances, it is difficult to determine whether magmatism has played a role in forming gold mineralization. OGDs and IRGDs (intrusion-related gold systems) form from similar ore fluids and have similar elemental or mineralogical characteristics except for Sn as the only metal that may be present in IRGDs but not in OGDs [66]. Tin minerals are not recorded from the above gold deposits. There is, however, at Pilgrim's Rest and Awak Mas a possible spatial and temporal relationship with igneous intrusions that may have been causative for the thermal disequilibrium with intruded host rock and the activation of the ore and alteration system [30–33,47–50].

Relevant questions related to the formation of OGDs encompass timing of mineralization relative to deformation and metamorphism. These data are summarized in Table 5. Gold mineralization is generally syn- to late-deformation [58,63]. Mesozonal deposits are typically syn- to post-peak greenschist facies and hypozonal types formed syn-to late-peak amphibolite facies metamorphism [1,63]. New Consort, Hutti, Hira Buddini and Navachab display two distinct stages of gold mineralization. Deposits related to igneous Intrusions are not directly connected to regional metamorphism.

Table 5. Hydrothermal alteration mineralogy.

Deposit	Alteration Assemblage
New Consort	1st stage: garnet, diopside, hornblende, K-feldspar, quartz, calcite, biotite
	2nd stage: hornblende, plagioclase, K-feldspar, biotite, quartz
Cuiabá	chlorite, carbonate, sericite, quartz, zoisite/clinozoisite
Ajjanahalli	chlorite, stilpnomelane, minnesotaite, sericite, ankerite
Renco	garnet, biotite, K-feldspar, quartz
Hutti	1st stage: biotite, chlorite, plagioclase.
	2nd stage: chlorite, K-feldspar
Hira Buddini	1st stage: biotite, K-feldspar, albite, actinolite, tourmaline, calcite
	2nd stage: muscovite, epidote, chlorite, quartz, calcite
Pilgrims's Rest	ferruginous carbonates, quartz, chlorite, sericite, rutile
Lega Dembi	actinolite, biotite chlorite, epidote, calcite, sericite, kyanite
Navachab	1st stage: garnet, diopside, quartz, K- feldspar.
	2nd stage: garnet, biotite
Mindyak	quartz, albite, sericite, chlorite, carbonates
Kochkar	biotite, actinolite, albite, K- feldspar, quartz, epidote, tourmaline
Awak Mas	sericite, calcite, epidote

Pressure-temperature conditions of mineralization are shown in Figure 3. Pressure-temperature estimates are based on detailed petrographic analyses of mineral assemblages and textures of host rocks and alteration zones. Orogenic gold deposits form in thermal equilibrium with their host rocks under similar P-T conditions to the metamorphosed

host [1,63]. P-T conditions were analyzed using several techniques. Conventional geothermometers and geobarometers were applied on suitable alteration mineral assemblages supported by phase-diagram modeling of TX pseudo-sections. Other P-T estimates were based on sulfide thermo-barometry, stable isotope thermometry, and pressure-corrected fluid inclusion data. P-T conditions record a range from 1 to 7 kbars and 215 to 680 °C. Most temperatures and pressures are in the range 1 to 3 kbars and 200 to 400 °C. The highest P-T conditions are observed for the first stage of mineralization at New Consort. The economic gold grade, however, is due to the second mineralization stage at 4.5 kbar and 590 °C. Two stages of gold mineralization are also recorded for Hutti and Hira Buddini. At both deposits the second mineralization stage with P-T conditions of 2 kbar and 350 °C is the most fertile gold producing stage.

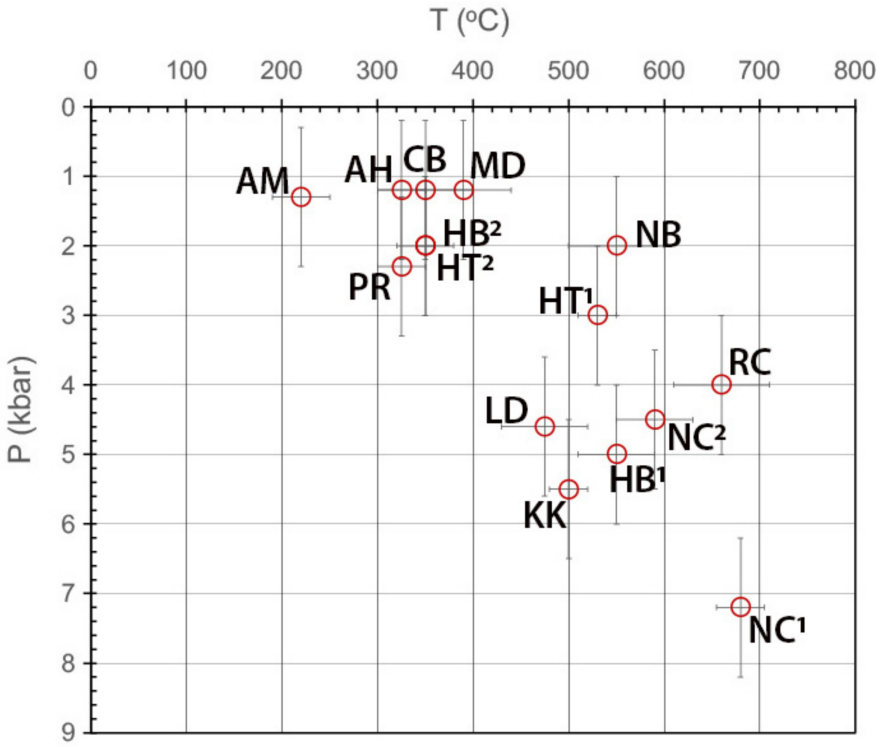

Figure 3. Pressure-temperature conditions of mineralization. Error bars indicate level of uncertainty. New Consort (NC^1, NC^2: 1st and 2nd stages of mineralization), Cuiabá, (CB) Ajjanahalli (AH), Renco (RC), Hutti (HT^1, HT^2), Hira Buddini (HB^1, HB^2), Lega Dembi (LD), Navachab (NB), Mindyak (MD), Kochkar (KK), Awak Mas (AW).

Figure 4 shows that temperature conditions for mesozonal mineralization are below the temperature range of main metamorphic fluid production in mafic bulk compositions while hypozonal deposits plot to the right of this temperature field [60]. The two stages of mineralization at Hutti and Hira Buddini are separated into the hypozonal and mesozonal areas with the latter representing the most productive second stage of ore formation. The conditions for the first stage of mineralization at New Consort and Renco plot close to the wet solidus line for granite, but below the wet solidus for the enderbite host rock at Renco and the amphibolite host at New Consort [1]. However, pegmatite dykes, suggestive of crustal anatexis, are associated with the ore zones in both deposits. Other deposits occupying the hypozonal field are Hutti, Hira Buddini, and Navachab. At Hutti and Hira Buddini the external magmatic fluid source originates from crustal derived pegmatites and granites, as is the case with the contemporaneous Kavital Granite. At Navachab magmatic activity evidenced by lamprophyre, pegmatite and aplite dykes overlap with the mineralization, and regional scale plutonism was coeval with deformation. The high

geothermal gradient and elevated fluid pressures indicate a hot, but relatively shallow-crustal hydrothermal system resulting from magmatic activity [35–40].

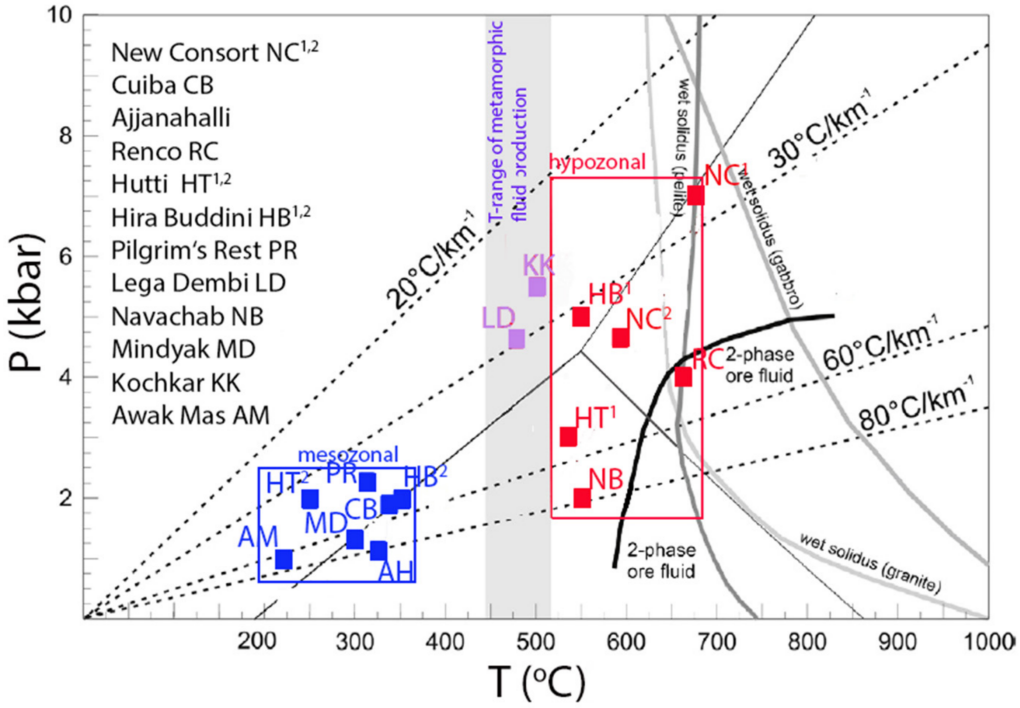

Figure 4. Pressure-temperature conditions of mineralization (modified from [1]). The fields for hypozonal and mesozonal orogenic gold deposits are delineated. Also included are geothermal gradients as well as wet solidi for granite, pelite, and gabbro. Errors are the same as in Figure 3.

Kochkar and Lega Dembi plot at an intermediate position in Figure 4. Gold mineralization at Kochkar formed at a mid-crustal level of a continental magmatic arc and post-dates active subduction and post orogenic plutonism. The lack of postcollisional collapse led to slow exhumation and a long-lasting cooling history, which triggered the fluid system responsible for gold mineralization [44–46]. Kochkar is not spatially associated with a transcrustal shear zone which differs markedly from other Phanerozoic orogenic gold settings [46]. At Lega Dembi, ore deposition occurred close to peak metamorphic conditions at lower-amphibolite metamorphic grades [34]. This is supported by the presence of kyanite along the margins of laminated quartz veins. The timing of metamorphism and fluid production was syn-to-late Pan-African orogeny and hence at the waning stages of the regional tectonism in the Adola granite-greenstone terrain [34]. The origin of ore fluids and age of formation at Awak Mas is contentious. A genetic relationship with a granodiorite intrusion at 8-6 was proposed by [47,48]. However, the deposit has also been classified as an epizonal OGD with a metamorphic fluid source [52]. Accordingly, rapid uplift after Miocene continental collision resulted in the metamorphic overprint of metasedimentary rocks during the retrogression stage accompanied by rock dehydration and ore fluid migration [52].

When considering typical hydrothermal alteration assemblages associated with orogenic gold mineralization a distinction is to be made between mesozonal and hypozonal types [56]. Mesozonal mineralization associated with greenschist facies metamorphism is generally accompanied by a proximal carbonate and sericite alteration and a distal zone characterized by chlorite. In contrast, hypozonal alteration can be more complex and varied in amphibolite facies terranes. Common assemblages associated with gold mineralization include garnet, biotite, amphibole, diopside, K-feldspar, plagioclase, calcite, and titanite. Alteration minerals seem to inherit their chemical signature from the host rocks and the alteration assemblages and mineralization are in general thermal equilibrium with the

country rocks [1,63]. There is a distinct mineralogical difference between the first and second alteration stages at New Consort, Hutti, Hira Buddini and Navachab. The different modal compositions are either related to different mineral stabilities at the prevailing differences in P-T conditions or differences in the hydrothermal fluid composition.

Principal gangue minerals in the orogenic gold lodes studied are quartz and carbonates together with variable amounts of sericite, chlorite, amphibole, biotite, scheelite, and tourmaline (Table 5).

Main ore minerals observed include native gold, pyrite, pyrrhotite, and minor amounts of chalcopyrite, arsenopyrite, tellurides, and bismuth minerals (Table 6). Sulfides typically constitute less than 10% of the ore with generally very low base metal sulfides. There is no general difference in the ore assemblages with mineralization ages. However, the occurrence of galena is restricted to Phanerozoic deposits and the presence of arsenopyrite together with loellingite is conspicuous in hypozonal deposits where arsenopyrite is the main sulfide. Sphalerite is a common constituent in almost all deposits but was not recorded at New Consort and Awak Mas. Native bismuth and bismuth minerals appear to be restricted to the hypozonal deposits New Consort, Renco and Navachab. The ore mineral assemblages determine the metal inventory of Au, As, Ag, Sb, Cu, Bi, Mo, Pb, S, W, Zn, but only gold is economically exploitable (Table 6). At New Consort, the simple ore assemblage of the low Au-grade first stage of mineralization consists of loellingite and pyrrhotite and is overprinted by the second stage of mineralization at conditions of 4.5 kbars and up to 590 °C. The mineralogy of this higher-grade gold ore is more complex including antimony and bismuth minerals. Gold fineness values reported for Cuiabá are in the range 759–941, for Kochkar 860–890, and for Awak Mas 920–940.

Table 6. Ore mineral assemblages.

Deposit	Ore Mineralogy
New Consort	1st stage: arsenopyrite, pyrrhotite, loellingite
	2nd stage: arsenopyrite, loellingite, pyrrhotite, chalcopyrite, pyrite, gold, ullmannite, stibnite, native antimony, bismuth, maldonite
Cuiabá	pyrite, pyrrhotite, arsenopyrite, chalcopyrite, sphalerite, gold
Ajjanahalli	pyrite, pyrrhotite, marcasite, arsenopyrite, chalcopyrite, sphalerite, gold
Renco	pryrite, pyrrhotite, chalcopyrite, sphalerite molybdenite, cubanite, magnetite ilmenite rutile, native bismuth, bismuth alloys, gold
Hutti	1st stage: pyrite, arsenopyrite, gold
	2nd stage: arsenopyrite, pyrrhotite, chalcopyrite, gold, scheelite
Hira Buddini	pyrite, chalcopyrite, magnetite, apatite, sphalerite, gold
Pilgrims's Rest	pyrite, arsenopyrite, fahlores, chalcopyrite, bismuthinite, native bismuth, gold
Lega Dembi	pyrite, pyrrhotite, arsenopyrite, chalcopyrite, galena, gersdorffite, sphalerite, tellurides, niccolite, bournonite, silvertetrahedrite, molybdenite, gold
Navachab	1st and 2nd stage: pyrrhotite, chalcopyrite, sphalerite, arsenopyrite, gold, bismuth, bismuthinite, bismuth tellurides, molybdenite, graphite
Mindyak	pyrite, arsenopyrite, chalcopyrite, sphalerite, galena
Kochkar	pyrite, arsenopyrite, chalcopyrite, sphalerite, tetradymite, gold, galena
Awak Mas	pyrite, galena, chalcopyrite, gold

Orogenic gold mineralization is typically associated with low salinity CO_2-H_2O-rich, near neutral pH hydrothermal fluids that are further characterized by the presence of H_2S, CH_4 and/or N_2 [65]. This fluid composition is regarded typical for mesozonal OGDs. The problem, however, is with hypozonal deposits that formed at conditions in excess of the optimal temperature range for metamorphic fluid production (Figure 4).

There is evidence that fluids forming the hypozonal mineralization at New Consort [3], Hutti [21], Hira Buddini [29], and Navachab [40] originated not only from metamorphic fluids but also from fluids that were released from crustal derived pegmatites and granites.

In the majority of the OGDs studied here, the conditions are such that phase separation (immiscibility or boiling) led to the development of salt-rich aqueous fluids coexisting with a volatile-rich phase (Table 7). In these deposits boiling is considered a major Au-depositing process. At Hutti, fluctuations in the fluid pressure stimulated phase separation, which initiated the precipitation of gold. Some of the laminated quartz veins contain gold up to 1000 g/t with visible gold co-precipitated with quartz. At Navachab fluid-pressure cycling during extensional fracturing has also been proposed to be the main trigger for gold mineralization in these veins. Fluid mixing played a role in the mineralization of the sediment-hosted deposits Pilgrim's Rest and Awak Mass.

Table 7. Isotopic signatures, physical conditions, and proposed origin of ore fluids.

	δ^{34}S (‰) Pyrite	δ^{18}O (‰) Quartz	δD (‰) Quartz	Fluid Salinity (wt. % $NaCl_{eq}$.)	Fluid Phase Separation	Fluid Origin
New Consort	-	-	-			magmatic/externally derived
Cuiabá	-	-	-			metamorphic
Ajjanahalli	+2.1–+2.7	13.6–14.4	$^{87}Sr/^{86}Sr$ (R_0) 0.7068–0.7078			mixed magmatic/metamorphic
Renco	-	7.8–9.2	-	2–10	+	magmatic/externally derived
Hutti	-	12.1–12.2	−51–−61	1–5	+	mixed magmatic/metamorphic
Hira Buddini	-	-	tourmaline δ^{11}B = −4–+9 ‰	0–21	+	mixed magmatic/metamorphic
Pilgrims's Rest	−2.8–+3.1	14.1–16.1	−51–−61	5–23	+	mixed contact metamorphism/basinal brines
Lega Dembi	-	-	$^{87}Sr/^{86}Sr$ (R_0) = 0.771	3–16	+	metamorphic
Navachab	+1.0–+8.3	12.2–17.9	−50–−55 ‰	4–16	+	mixed magmatic/metamorphic
Mindyak	+1.0–+4.1	18.2–21.5	calcite δ^{13}C = −5.31–−7.63,	3–7	+	metamorphic
Kochkar		10.5–11.8	$^{87}Sr/^{86}Sr$ (R_0) = 0.7093	11–14	+	Mixed magmatic/metamorphic
Awak Mas	−6.6–+12.9	10.2–12.7	-	2–6	+	metamophic

Oxygen and deuterium isotope data are ambiguous as the data range of magmatic and metamorphic fluids overlap, and there is no simple distinction possible between both fluid sources [67]. This means that constraining the fluid origin on stable isotope data only could be erroneous, but the interpretations made from isotope data in this paper are supported by published data on geochemistry, mineralogy, petrography, and fluid inclusions. Some deposits studied are related to intrusions and overlap in age with magmatic events. In this case, a mixed magmatic–hydrothermal model may be most appropriate for explaining the source of metals and fluids.

This ambivalence related to the source is displayed in the data set in Table 7. The mesozonal OGDs Cuiabá, Lega Dembi, and Mindyak are assumed to have a metamorphic fluid source. The mixed metamorphic-magmatic model seems to be more appropriate for New Consort, Hutti, and Navachab. Pilgrim's Rest and Awak Mas are hosted by thick low-grade sedimentary successions which may exclude a metamorphic contribution to the ore fluid from the host sedimentary pile. A scenario that invokes a magmatic heat source and a mixture of magmatic fluids and formation waters is regarded the best model.

Mean δD and δ^{18}O values for ore-forming fluids calculated for Hutti, Pilgrim's Rest and Navachab are shown in Figure 5.

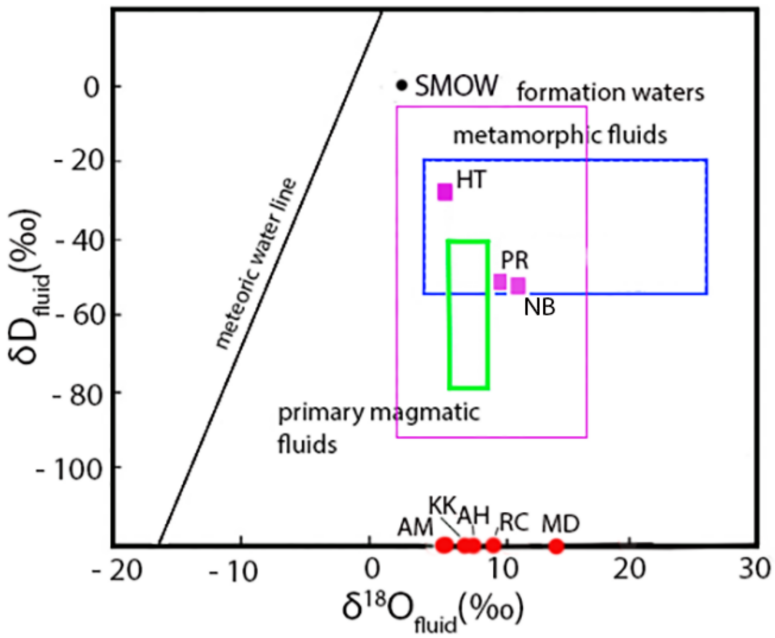

Figure 5. Plot of δD versus $\delta^{18}O$ fluid data compared to fluids of different origin. Modified from [68]. (HT-Hutti; PR-Pilgrim's Rest; NB-Navachab, AM-Awak Mas; KK-Kochkar; AH-Ajjanahalli; RC-Renco; MD-Mindyak).

The $\delta^{18}O$ and δD compositions for Hutti, Pilgrim's Rest and Navachab occupy the field of metamorphic fluids whereby the Hutti $\delta^{18}O$ fluid value plots to the left of the primary magmatic fluid field. The Pilgrim's Rest and Navachab $\delta^{18}O$ fluid values are slightly heavier than magmatic fluids but their δD fluid data plot close to the lower boundary of the metamorphic fluid field. The isotope data are equivocal, but they do not militate against a mixed magmatic-metamorphic fluid origin as was proposed for Hutti. Pilgrim's Rest, Navachab and Awak Mas are hosted by sediments like dolomite and carbonaceous shale and banded marble and biotite shists. Thus, it is likely that the fluids were magmatic in origin and exchanged their isotopic signature with that of the host successions. As for the remaining deposits δD data are not available, their mean $\delta^{18}O$ fluid values are plotted on the $\delta^{18}O$ axis in Figure 5. Mindyak has the heaviest mean $\delta^{18}O$ fluid value, and the fluid is regarded of metamorphic origin. Awak Mas, Kochkar, Ajjanahalli and Renco straddle the $\delta^{18}O$ range defined by magmatic, metamorphic and formation waters. While at Awak Mas the ore fluid is probably a mixture of formation waters and magmatic fluids, the data for Kochkar and Ajjanahalli suggest a deep magmatic and metamorphic fluid source. The ore fluid as Renco was externally derived from devolatilization of the overthrusted greenstone terrane of the Zimbabwe Craton.

Economic data such as gold reserves, production and grade are summarized in Table 8 The high demand for and price of gold and innovative mining technology has encouraged mining companies to engage in the exploitation of deposits that previously deemed too difficult or expensive. For example, the Navachab open cast operation produces gold from ore with an average grade of 1.29 g/t but the ore tonnage is of a magnitude like that of many high tonnage-low grade porphyry copper deposits. Because of the presence of native gold in some deposits like New Consort, Hutti, and Pilgrim's Rest ore grades can be highly variable with up to 10 kg/t of gold locally while on a mining level mean economic grades of 5–19 g/t are obtained. However, none of the single deposits discussed here reaches the status of a world-class or giant deposit which according to the threshold proposed by [69] should have contained gold of at least 100 metric tons (3.2 Moz). Only the goldfields at Barberton (320 t), Pilgrim's Rest (186 t), Kochkar (about 300 t) and Hutti (ca. 100 t) are in the league of giant gold producers. When Navachab is excluded from the calculation, a negative trend is observable between ore tonnage und grade. Ore reserves of producing

mines are, however, dependent on exploration activities and represent dynamic figures that change with demand and commodity price.

Table 8. Gold reserve, production, and grade.

Deposit	Ore Reserves (Mt) (Proven & Probable)	Historic Au Production (t)	Annual Au Production (kg)	Au Grade (g/t)
New Consort	1.41	59.54	340.2	9.4
Cuiabá	7.89			4.68
Ajjanahalli	7.34	(1995–2002) 0.963		1.43
Renco	2.90			6.03
Hutti	9.25	89.59		5.62
Hira Buddini	0.51			4.16
Pilgrim's Rest	45.5	(1872–1972) 168	(1999–2014) 284	4.17
Lega Dembi Closed 2018	20.8	77		3.71
Navachab	45.3	35.29	1501	1.29
Mindyak closed	12.2	30.1		2.5
Kochkar	10.7	300		4.9
Awak Mas	20.2			1.58

3. Discussion and Conclusions

If OGDs define a coherent group of mineralization types, the same general processes should always have been in operation for the formation of OGDs of all ages and geologic setting. On a deposit scale, the set of OGDs presented here reveal distinct differences with respect to the time-lag between age of host rock and gold mineralization, geologic setting, nature of host rocks, pressure-temperature conditions of ore formation, source of fluids, ore- and alteration mineralogy and metal association. The common feature among the deposits discussed here is that gold mineralization is predominantly confined to often laminated quartz-carbonate veins and that they are gold-only deposits because only gold is economically exploitable. Other similarities include the chemistry of ore fluids which does not significantly differ with mineralization age or geologic setting and the syn- to post-peak metamorphic timing of mineralization.

The formation of giant orogenic gold mineral systems is explained by a model where gold is sourced from devolatilization of pyritic sediments above a subducting slab of oceanic crust [70–72]. In this model, fluids and metals are sourced from below the craton or released from mantle lithosphere that was metasomatized and fertilized during a subduction event. In this context, the crustal metamorphic model which proposes that orogenic gold formed late in regional metamorphism from deep-crustal metamorphic fluids is regarded less likely. In the crustal metamorphic model, the source rocks would be part of the craton where mineralization occurred. The problem with this model is that hypozonal gold deposits formed under amphibolite to lower granulite facies conditions would have to be considered anomalous exceptions [70,71]. Furthermore, magmatic hydrothermal models also seem to fail because of the commonly observed lack of temporal and spatially associated granitic intrusions [70–72].

This orogenic gold system model defines useful parameters for the search for world-class OGDs or well-endowed mineral provinces [63,65,72,73]. However, most of the deposits discussed here are situated in less-endowed orogenic gold provinces or in areas where they are the only gold know gold deposit like Renco, Navachab, or Ajjanahalli. This may explain the deviation of their genetic signatures from the model parameters proposed for giant OGDs. For example, a two-stage mineralization event by different fluids is not considered by the crustal metamorphic model. However, two stages of gold-depositional processes were significant at New Consort, Hutti, Hira Buddini, and Navachab with the second stage fluids being the principal gold carriers. Furthermore, there is evidence, in

some cases from boron and strontium isotopes, supporting the involvement of a mixture of metamorphic and magmatic sourced ore fluids such as at Ajjanahalli, Hutti, Hira Buddini, Pilgrim's Rest. Navachab, and Kochkar. At Navachab the intrusion of lamprophyre, granite pegmatite and aplite dykes are coeval with mineralization [36]. Pegmatites and aplites pointing to a crustal source, but lamprophyre dikes may reflect the mantle connectivity of controlling first-order structures [71].

The ore mineral assemblages recognized determine the metal inventory of Au, As, Ag, Sb, Cu, Bi, Mo, Pb, S, W, and Zn. The occurrence of galena is restricted to Phanerozoic deposits and the presence of arsenopyrite together with loellingite is conspicuous in hypozonal deposits where arsenopyrite is the main sulfide. Sphalerite is a common constituent in almost all deposits but was not recorded at New Consort and Awak Mas. Native bismuth and bismuth minerals appear to be restricted to the hypozonal deposits New Consort, Renco and Navachab.

The salinity of metamorphic OGD ore fluids is generally low, with 3–7 wt.% NaCl equiv. [70]. This is a distinct characteristic of gold-only deposits, because low salinity fluids facilitate the decoupling of Au from base metals by the partitioning of Au into the auriferous fluid, without the base metals Cu, Pb and Zn [74]. However, experimental results [75] provide indirect support for a magmatic component in fluids forming OGDs. The experiments [75] showed that CO_2-rich magmatic fluids that exsolve early or at greater depth from ascending hydrous magmas suppress fluid salinity and thus facilitate the formation of base-metal-poor but gold-rich fluids, as observed in OGD formation associated with late granitoid intrusions. The salinity values recorded for Hutti, Renco, Mindyak and Awak Mass fall in the range of most OGDs and a mixed methamorphic-magmatic fluid source appears feasible. The fact, that Hira Buddini, Pilgrim's Rest, Lega Dembi, Navachab and Kochkar have ore fluid salinities that are outside the common range of OCDs does not contradict a mixed magmatic-metamorphic fluid source. This opens the question if the gold-base metal decoupling process advocated by [74] is the only possible explanation for gold-only deposits or if fluid sources and base metal availability equally play a role. For example, experimental work and modeling carried out by [75] demontrate that in melts that begin degassing at a late stage of differentiation decoupling of copper and chlorine is due to the relatively higher fluid/melt partition coefficient for copper compared to chlorine. Additionally, the presence of reduced sulphur in the melt may promote sulphide saturation that inhibits copper enrichment in the residual melt.

The orogenic gold system model [70–72] advocates a metal and fluid source external to the terrain in which mineralization occurred. Here, externally sourced ore fluids are suggested only for New Consort, Renco and possibly Navachab. All other deposits most likely formed from a crustal source, which would favor the crustal metamorphic model.

However, the formation of hypozonal mineralization cannot be accounted for by the crustal metamorphic model. It has been proposed [1] that they formed in evolved accretionary or collisional orogens, where nappe stacking or extensional unroofing generated P-T gradients and structures that promoted fluid migration. The ore fluid was sourced either by metamorphic devolatilization at lower metamorphic grades or represent mixtures of high-temperature metamorphic and magmatic fluids, the latter being derived from anatectic granites and pegmatites [1].

Obviously, neither the orogenic gold system model nor the crustal metamorphic model can provide adequate explanations for all facets of OGDs formation. Although OGDs do have to certain extent a set of coherent signatures but there seem to be no unified model for all possible environmental conditions and facets of ore formation and fluid source, tectonic and lithologic setting, and scale of gold endowment.

Funding: This research received no external funding.

Data Availability Statement: Data are available in the refrences cited.

Acknowledgments: This manuscript grew out of research that the author conducted with colleagues and PhD students on a large number of orogenic gold deposits in various parts of the world. I would

like to extend particular thanks to Annika Dziggel, Alex Kisters and Jochen Kolb for their invaluable contributions, knowledge and insights into this complex type of gold deposits. The manuscript benefited from critical reviews by three anonymous reviewers. Financial support by the Deutsche Forschungsgemeinschaft (DFG grant Me 1425/1-1 to ME 1425/13-1) and the German Academic Exchange Service (DAAD) is gratefully acknowledged.

Conflicts of Interest: The author declares no conflict of interest.

References

1. Kolb, J.; Dziggel, A.; Bagas, L. Hypozonal lode gold deposits: A genetic concept based on a review of the New Consort, Renco, Hutti, Hira Buddini, Navachab, Nevoria and The Granites deposits. *Precambrian Res.* **2015**, *262*, 20–44. [CrossRef]
2. Dziggel, A.; Poujol, M.; Otto, A.; Kisters, A.F.M.; Trieloff, M.; Schwarz, W.; Meyer, F.M. New U–Pb and 40Ar/39Ar ages from the northern part of the Barberton greenstone belt, South Africa: Implications for the formation of Mesoarchaean gold deposits. *Precambrian Res.* **2010**, *179*, 206–220. [CrossRef]
3. Dziggel, A.; Otto, A.; Kisters, A.F.M.; Meyer, F.M. Tectono-metamorphic controls on Archaean gold mineralization in the Barberton greenstone belt. South Africa: An example from the New Consort gold mine. In *Earth's Oldest Rocks. Developments in Precambrian Geology*; Van Kranendonk, M.J., Smithies, R.H., Bennet, V., Eds.; Elsevier: Amsterdam, The Netherlands, 2007.
4. Dziggel, A.; Knipfer, S.; Kisters, A.F.M.; Meyer, F.M. P–T and structural evolution during exhumation of high-T, medium-P basement rocks in the Barberton Mountain Land, South Africa. *J. Metamorph. Geol.* **2006**, *24*, 535–551. [CrossRef]
5. Dziggel, A.; Stevens, G.; Poujol, M.; Anhaeusser, C.R.; Armstrong, R.A. Metamorphism of the granite-greenstone terrane to the south of the Barberton greenstone belt, South Africa: An insight into the tectono-thermal evolution of the lower portions of the Onverwacht Group. *Precambrian Res.* **2002**, *114*, 221–247. [CrossRef]
6. Kisters, A.F.; Belcher, R.W.; Poujol, M.; Dziggel, A. Continental growth and convergence-related arc plutonism in the Mesoarchaean: Evidence from the Barberton granitoid-greenstone terrain, South Africa. *Precambrian Res.* **2010**, *178*, 15–26. [CrossRef]
7. Kisters, A.F.M.; Stevens, G.; Dziggel, A.; Armstrong, J.T. Extensional detachment faulting at the base of the Barberton greenstone belt: Evidence for a 3.2 Ga orogenic collapse. *Precambrian Res.* **2003**, *127*, 355–378. [CrossRef]
8. Otto, A.; Dziggel, A.; Kisters, A.F.M.; Meyer, F.M. The New Consort Gold Mine, Barberton greenstone belt, South Africa: Orogenic gold mineralization in a condensed metamorphic profile. *Miner. Depos.* **2007**, *42*, 715–735. [CrossRef]
9. Otto, A. Tektono-Metamorphe Kontrolle der Archaischen Goldmineralisation in der New Consort Gold Mine, Barberton Grünsteingürtel, Südafrika. Ph.D. Thesis, RWTH Aachen University, Aachen, Germany, 1997; 160p. Available online: https://publications.rwth-aachen.de/record/50397/files/Otto_Alexander.pdf (accessed on 20 January 2023).
10. Ribeiro-Rodrigues, L.C.; Gouveia de Oliveira, C.; Friedrich, G. The Archean BIF-hosted Cuiabá Gold deposit, Quadrilátero Ferrífero, Minas Gerais, Brazil. *Ore Geol. Rev.* **2007**, *32*, 543–570. [CrossRef]
11. Lobato, L.M.; Ribeiro-Rodrigues, L.C.; Vieira, F.W.R. Brazil's premier gold province. Part II: Geology and genesis of gold deposits in the Archean Rio das Velhas greenstone belt, Quadrilátero Ferrífero. *Miner. Depos.* **2001**, *36*, 249–277. [CrossRef]
12. Ribeiro-Rodrigues, L.C.; Friedrich, G.; Meyer, F.M. The Cuiabá gold deposit, Minas Gerais, Brazil. *Erzmetall (World Min.)* **1999**, *52*, 424–437.
13. Ribeiro-Rodrigues, L.C. Gold in Archaen banded ironformation of the Quadrilátero Ferrífero, Minas Gerais, Brazil—The Cuiabá Mine. Ph.D. Thesis, RWTH Aachen University, Aachen, Germany, 1998; 264p. Band 27.
14. Kolb, J.; Hellmann, A.; Rogers, A.; Sindern, S.; Vennemann, T.; Böttcher, M.E.; Meyer, F.M. The Role of a Transcrustal Shear Zone in Orogenic Gold Mineralization at the Ajjanahalli Mine, Dharwar Craton, South India. *Econ. Geol.* **2004**, *99*, 743–759. [CrossRef]
15. Sarma, D.S.; Fletcher, I.R.; Rasmussen, B.; McNaughton, N.J.; Mohan, M.R.; Groves, D.I. Archaean gold mineralization synchronous with late cratonization of the Western Dharwar Craton, India: 2.52 Ga U–Pb ages of hydrothermal monazite and xenotime in gold deposits. *Miner. Depos.* **2011**, *46*, 273–288. [CrossRef]
16. Kisters, A.F.M.; Kolb, J.; Meyer, F.M.; Hoernes, S. Hydrologic segmentation of high-temperature shear zones: Structural, geochemical, and isotopic constraints from auriferous mylonites of the Renco Mine, southern Zimbabwe. *J. Struct. Geol.* **2000**, *22*, 811–829. [CrossRef]
17. Kisters, A.F.M.; Kolb, J.; Meyer, F.M. Gold mineralization in high-grade metamorphic shear zones of the Renco Mine, southern Zimbabwe. *Econ. Geol.* **1998**, *93*, 587–601. [CrossRef]
18. Kolb, J.; Kisters, A.F.M.; Meyer, F.M.; Siemes, H. Polyphase deformation of mylonites of the Renco gold mine, Northern Marginal Zone, Limpopo Belt, Zimbabwe: Identified by crystallographic preferred orientation of quartz. *J. Struct. Geol.* **2003**, *25*, 253–262. [CrossRef]
19. Kolb, J.; Meyer, F.M. Fluid inclusion record of the hypozonal orogenic Renco gold deposit (Zimbabwe) during the retrograde P–T evolution. *Contrib. Mineral. Petrol.* **2002**, *143*, 495–509. [CrossRef]
20. Kolb, J.; Kisters, A.F.M.; Hoernes, S.; Meyer, F.M. The origin of fluids and nature of fluid-rock interaction in auriferous mylonites of the Renco Mine, southern Zimbabwe. *Miner. Depos.* **2000**, *35*, 109–125. [CrossRef]
21. Rogers, A.J.; Kolb, J.; Meyer, F.M.; Vennemann, T. Two stages of gold mineralization at Hutti mine, India. *Miner. Depos.* **2012**, *48*, 99–114. [CrossRef]

22. Kolb, J.; Meyer, F.M. Balanced mineral reactions for alteration zones developed in auriferous shear zones of the Hutti Mine, Dharwar Craton, India. *Z. Dtsch. Ges. Geowiss* **2008**, *159*, 331–347. [CrossRef]
23. Rogers, A.; Kolb, J.; Meyer, F.; Armstrong, R. Tectono-magmatic evolution of the Hutti-Maski Greenstone Belt, India: Constrained using geochemical and geochronological data. *J. Asian Earth Sci.* **2007**, *31*, 55–70. [CrossRef]
24. Rogers, A.J. Petrological, Geochemical and Stable Isotope Characterization of Auriferous Shear Zones at the Hutti-Maski Gold Mine, Dharwar Craton, India. Ph.D. Thesis, RWTH Aachen University, Aachen, Germany, 2005; 275p. Band 40.
25. Rogers, A.; Kolb, J.; Meyer, F.M. P-T conditions and fluid evolution in the Hutti Gold Mine, India. *Ber. Der Dtsch. Mineral.Ges. Suppl. Eur. J. Mineral.* **2002**, *14*, 138.
26. Kolb, J.; Rogers, A.; Meyer, F.M. Relative timing of deformation and two-stage gold mineralization at Hutti mine, Dharwar Craton, India. *Miner. Depos.* **2005**, *40*, 156–174. [CrossRef]
27. Kolb, J.; Rogers, A.; Meyer, F.; Vennemann, T.W. Development of fluid conduits in the auriferous shear zones of the Hutti Gold Mine, India: Evidence for spatially and temporally heterogeneous fluid flow. *Tectonophysics* **2004**, *378*, 65–84. [CrossRef]
28. Hellmann, A. Die Genese der Goldlagerstätte Hira Buddini, Südindien. Ph.D. Thesis, RWTH Aachen University, Aachen, Germany, 2009; 351p. Available online: https://publications.rwthaachen.de/record/50139/files/Hellmann_Andre.pdf (accessed on 10 January 2023).
29. Krienitz, M.-S.; Trumbull, R.B.; Hellmann, A.; Kolb, J.; Meyer, F.M.; Wiedenbeck, M. Hydrothermal gold mineralization at the Hira Buddini gold mine, India: Constraints on fluid evolution and fluid sources from boron isotopic compositions of tourmaline. *Miner. Depos.* **2008**, *43*, 421–434. [CrossRef]
30. Meyer, F.M.; Robb, L.J. The geochemistry of black shales from the Chuniespoort Group, Transvaal Sequence, eastern Transvaal, South Africa. *Econ. Geol.* **1996**, *91*, 111–121. [CrossRef]
31. Meyer, F.M.; Welke, H.J.; Robb, L.J. Mineralogical and chemical characteristics of flat reefs in the Sabie-Pilgrim's Rest Goldfield. In *Geocongress'86*; The Geological Society of South Africa: Marshalltown, South Africa, 1986; pp. 535–540.
32. Summer, D.Y.; Bowring, S.A. U-Pb geochronologic constraints on deposition of the Campbellrand Subgroup, Transvaal Supergroup, South Africa. *Precambrian Res.* **1996**, *79*, 25–35. [CrossRef]
33. Boer, R.H.; Meyer, F.M.; Robb, L.J.; Graney, J.R.; Vennemann, T.W.; Kesler, S.E. Mesothermal-typ mineralization in the Sabie-Pilgrim's Rest Goldfield, South Africa. *Econ. Geol.* **1995**, *90*, 860–876. [CrossRef]
34. Billay, A.Y.; Kisters, A.F.M.; Meyer, F.M.; Schneider, J. The geology of the Lega Dembi gold deposit, southern Ethiopia: Implications for Pan-African gold exploration. *Miner. Depos.* **1997**, *32*, 491–504. [CrossRef]
35. Wulff, K. Petrography, Geochemistry, and Stable Isotope Characteristics of the Navachab Gold Deposit, Namibia. Ph.D. Thesis, RWTH Aachen University, Aachen, Germany, 2008; 203p. Available online: https://publications.rwth-aachen.de/record/50787/files/Wulff_Katharina.pdf (accessed on 1 January 2023).
36. Dziggel, A.; Wulff, K.; Kolb, J.; Meyer, F. Processes of high-T fluid–rock interaction during gold mineralization in carbonate-bearing metasediments: The Navachab gold deposit, Namibia. *Miner. Depos.* **2009**, *44*, 665–687. [CrossRef]
37. Dziggel, A.; Wulff, K.; Kolb, J.; Meyer, F.M.; Lahaye, Y. Significance of oscillatory and bell-shaped growth zoning in hydrothermal garnet: Evidence from the Navachab gold deposit, Namibia. *Chem. Geol.* **2009**, *262*, 262–276. [CrossRef]
38. Kisters, A.F.M. Controls of gold-quartz vein formation during regional folding in amphibolite-facies, marble dominated metasediments of the Navachab Gold Mine in the Pan-African Damara Belt, Namibia. *S. Afr. J. Geol.* **2005**, *108*, 365–380. [CrossRef]
39. Kisters, A.F.; Jordaan, L.; Neumaier, K. Thrust-related dome structures in the Karibib district and the origin of orthogonal fabric domains in the south Central Zone of the Pan-African Damara belt, Namibia. *Precambrian Res.* **2004**, *133*, 283–303. [CrossRef]
40. Wulff, K.; Dziggel, A.; Kolb, J.; Vennemann, T.; Böttcher, M.E.; Meyer, F.M. Origin of Mineralizing Fluids of the Sediment-Hosted Navachab Gold Mine, Namibia: Constraints from Stable (O, H, C, S) Isotopes. *Econ. Geol.* **2010**, *105*, 285–302. [CrossRef]
41. Chugaev, A.; Znamensky, S.E. Lead Isotope Characteristics of the Mindyak Gold Deposit, Southern Urals: Evidence for the Source of Metals. *Geol. Ore Depos.* **2018**, *60*, 52–61. [CrossRef]
42. Ertl, R.G.W.; Znamensky, S.; Kisters, A.F.M.; Meyer, F.M.; Seravkin, I.B.; Kosarev, A.M. The Mindyak gold deposit in the southern Urals, Russia—A mineralization between epi- and mesozonal levels. EUG Abstract supplement no. 1. *Terra Nova* **1999**, *10*, 764.
43. Kisters, A.F.M.; Meyer, F.M.; Seravkin, I.B.; Znamenski, S.N.; Kosarev, A.M.; Ertl, R.G.W. The geological setting of lode-gold deposits in the central south Urals: A review. *Geol. Rundschau* **1999**, *87*, 603–616. [CrossRef]
44. Kolb, J.; Sindern, S.; Kisters, A.F.M.; Meyer, F.M.; Hoernes, S.; Schneider, J. Timing of Uralian orogenic gold mineralization at Kochkar in the evolution of the East Uralian granite-gneiss terrane. *Miner. Depos.* **2005**, *40*, 473–491. [CrossRef]
45. Kisters, A.F.M.; Meyer, F.M.; Znamensky, S.E.; Seravkin, I.B.; Ertl, R.G.W.; Kosarev, A.M. Structural controls of lode-gold mineralization by mafic dykes in late-Paleozoic granitoids of the Kochkar district, southern Urals, Russia. *Miner. Depos.* **2009**, *35*, 157–168. [CrossRef]
46. Kisters, A.F.M.; Meyer, F.M.; Znamensky, S.E.; Seravkin, I.B.; Ertl, R.G.W.; Kosarev, A. Dyke-shear zone relationships in late-Paleozoic granitoids of the Plast massif and their significance for lode-gold mineralization in the Kochkar district, southern Urals, Russia. *Econ. Geol. Res. Unit Inf. Circular* **1999**, *335*, 1–19.
47. Ernowo, E.; Idrus, A.; Meyer, F.M. Elemental Gains and Losses during Hydrothermal Alteration in Awak Mas Gold Deposit, Sulawesi Island, Indonesia: Constraints from Balanced Mineral Reactions. *Minerals* **2022**, *12*, 1630. [CrossRef]
48. Ernowo, E.; Meyer, F.M.; Idrus, A. Hydrothermal alteration and gold mineralization of the Awak Mas metasedimentary rock-hosted gold deposit, Sulawesi, Indonesia. *Ore Geol. Rev.* **2019**, *113*, 103083. [CrossRef]

49. Ernowo, E. Hydrothermal Alteration and Gold Mineralization of the Awak Mas Gold Deposit, Sulawesi Island, Indonesia. Ph.D. Thesis, RWTH Aachen University, Aachen, Germany, 2017; 200p.
50. Ernowo, E.; Meyer, F.M.; Idrus, A. Hydrothermal alteration and gold mineralization of the meta-sedimentary rock hosted gold deposit Awak Mas, Sulawesi Island, Indonesia. In Proceeding of the 35th International Geological Congress, Cape Town, South Africa, 27 August–4 September 2016.
51. Ernowo, E.; Meyer, F.M.; Idrus, A.; Widyanarko, H.; Endrasari, N.L. An update of key characteristics of Awak Mas mesothermal gold deposit, Sulawesi Island, Indonesia. In Proceedings of the MGEI Annual Meeting, Bandung, Indonesia, 4–6 October 2016.
52. Hakim, A.Y.; Melcher, F.; Prochaska, W.; Bakker, R.; Rantitsch, G. Formation of epizonal gold mineralization within the Latimojong Metamorphic Complex, Sulawesi, Indonesia: Evidence from mineralogy, fluid inclusions and Raman spectroscopy. *Ore Geol. Rev.* **2018**, *97*, 88–108. [CrossRef]
53. White, L.T.; Hall, R.; Armstrong, R.A.; Barber, A.J.; Fadel, M.B.; Baxter, A.; Wakita, K.; Manning, C.; Soesilo, J. The geological history of the Latimojong region of western Sulawesi, Indonesia. *J. Asian Earth Sci.* **2017**, *138*, 72–91. [CrossRef]
54. Gaboury, D. Parameters for the formation of orogenic gold deposits. *Appl. Earth Sci.* **2019**, *128*, 124–133. [CrossRef]
55. Groves, D.I.; Goldfarb, R.J.; Gebre-Mariam, M.; Hagemann, S.G.; Robert, F. Orogenic gold deposits: A proposed classification in the context of their crustal distribution and relationship to other gold deposit types. *Ore Geol. Rev.* **1998**, *13*, 7–27. [CrossRef]
56. Gebre-Mariam, M.; Hagemann, S.G.; Groves, D.I. A classification scheme for epigenetic Archaean lode-gold deposits. *Miner. Depos.* **1995**, *30*, 408–410. [CrossRef]
57. Groves, D.I. The crustal continuum model for late-Archaean lode-gold deposits of the Yilgarn Block, Western Australia. *Miner Depos.* **1993**, *28*, 366–374. [CrossRef]
58. Hagemann, S.G.; Cassidy, K.F. Archean orogenic lode gold deposits. In *Gold in 2000: Reviews in Economic Geology*; Hagemann, S.G., Brown, P.E., Eds.; Society of Economic Geologists: Littleton, CO, USA, 2000; pp. 9–68.
59. Bierlein, F.P.; Groves, D.I.; Cawood, P.A. Metallogeny of accretionary orogens—The connection between lithospheric processes and metal endowment. *Ore Geol. Rev.* **2009**, *36*, 282–292. [CrossRef]
60. Phillips, G.N.; Powell, R. Formation of gold deposits: A metamorphic devolatilization model. *J. Metam. Geol.* **2010**, *28*, 689–718. [CrossRef]
61. Connolly, J.A.D. The mechanics of metamorphic fluid expulsion. *Elements* **2010**, *6*, 165–172. [CrossRef]
62. Phillips, G.N.; Powell, R. Formation of gold deposits: Review and evaluation of the continuum model. *Earth-Sci. Rev.* **2009**, *94*, 1–21. [CrossRef]
63. Groves, D.I.; Santosh, M.; Zhang, L. A scale-integrated exploration model for orogenic gold deposits based on a mineral system approach. *Geosci. Front.* **2020**, *11*, 719–738. [CrossRef]
64. Bogossian, J.; Kemp, A.I.S.; Hagemann, S.G. Linking Gold Systems to the Crust-Mantle Evolution of Archean Crust in Central Brazil. *Minerals* **2021**, *11*, 944. [CrossRef]
65. Goldfarb, R.J.; Groves, D.I. Orogenic gold: Common vs evolving fluid and metal sources through time. *Lithos* **2015**, *233*, 2–26. [CrossRef]
66. Hart, C.J.R.; Mair, J.L.; Goldfarb, R.J.; Groves, D.I. Source and Redox Controls of Intrusion-RelatedMetallogeny, Tombstone-Tungsten Belt, Yukon, Canada. In *Fifth Hutton Symposium Volume, Transactions of the Royal Society of Edinburgh: Edinburgh Earth Sciences*; Cambridge University Press: Cambridge, UK, 2004; pp. 339–356.
67. Ridley, J.R.; Diamond, L.W. Fluid chemistry of orogenic lode gold deposits and implications for genetic models. *Rev. Econ. Geol.* **2000**, *13*, 141–162. [CrossRef]
68. Hoefs, J. *Stable Isotope Geochemistry*; Springer: Berlin, Germany, 2009.
69. Singer, D.A. World class base and precious metal deposits; a quantitative analysis. *Econ. Geol.* **1995**, *90*, 88–104. [CrossRef]
70. Goldfarb, R.J.; Groves, D.I.; Gardoll, S. Orogenic gold and geologic time: A global synthesis. *Ore Geol. Rev.* **2001**, *18*, 1–75. [CrossRef]
71. Hronsky, J.M.A.; Groves, D.I.; Loucks, R.R.; Begg, G.C. A unified model for gold mineralisation in accretionary orogens and implications for regional-scale exploration targeting methods. *Miner. Depos.* **2012**, *47*, 339–358. [CrossRef]
72. Groves, D.I.; Goldfarb, R.J.; Santosh, M. The conjunction of factors that lead to formation of giant gold provinces and deposits in non-arc settings. *Geosci. Front.* **2015**, *7*, 303–314. [CrossRef]
73. Groves, D.I.; Santosh, M.; Deng, J.; Wang, Q.; Yang, L.; Zhang, L. A holistic model for the origin of orogenic gold deposits and its implications for exploration. *Miner. Depos.* **2019**, *55*, 275–292. [CrossRef]
74. Phillips, G.N.; Powell, R. A practical classification of gold deposits, with a theoretical basis. *Ore Geol Rev.* **2015**, *65*, 568–573. [CrossRef]
75. Hsu, Y.-J.; Zajacz, Z.; Ulmer, P.; Heinrich, C.A. Chlorine partitioning between granitic melt and H_2O-CO_2-NaCl fluids in the Earth's upper crust and implications for magmatic-hydrothermal ore genesis. *Geochim. Cosmochim. Acta* **2019**, *261*, 171–190. [CrossRef]